E1e - Basic Electric Circuits

Lab Group 6: Jordan Grey([redacted])*(50%)*, ([redacted])*(50%)*

December 10, 2024

Abstract

This report evaluates the experimental results an variety circuits with both linear and non-linear fitting techniques to compare and contrast the discrepancies between theoretical and experimental results. For Task I, the series circuit demonstrated a near-perfect linear relationship ($r^2 = 0.9998$) for the line with slope $a = 0.00413$ and intercept $b = -0.05$. The parallel circuit deviated from linearity, with a notable inconsistency suggesting experimental error and a best fit with $r^2 = 0.81$. Task II examined a voltage divider circuit and analyzed deviations in R_L values due to internal resistances, with a $R_1 = 110.76\Omega$ and $\frac{R_1}{R_2} = 0.11$. The Wheatstone Bridge results showed a strong correlation of $r^2 = 0.9862$ and $r^2 = 0.99774$ for theoretical and fitted comparisons with experimental data. experimental comparison to R_2 was inconclusive due to high relative uncertainties in both theoretical and physically measured results. Enhanced precision in components and methods is recommended for future studies. The High Pass Filter task aligned well with theoretical expectations at high frequencies ($r^2 = 0.99823$), but impedance mismatches caused discrepancies at lower frequencies. Improved experimental setups using PCB boards and precise components are suggested to enhance reliability. Additionally the results of the non-linear fitting yielded valuable conclusions due to the propagation of error through a complex valued function.

1 Introduction

In this report, a series of fundamental electrical circuits were constructed and analyzed to explore key concepts, including Ohm's Law, Kirchoff's Rules, the concept of and there applications to Series and Parallel circuits, the Voltage Divider circuit, the Wheatstone Bridge circuit and the High Pass Filter circuit. The theoretical expectations for each circuit was explored and compared with the experimental results taking into consideration uncertainty from factors such as internal resistances of wires, digital measuring equipment and component tolerances, in an effort to gain a deeper understanding of the practical aspects of circuit design and measurement.

2 Theoretical Basis

2.1 Basic Circuits

In a series circuit, the equivalent resistance is the sum of the individual resistances:

$$R_{\text{eq}_s} = \sum_{i=1}^{n} R_i \tag{1}$$

The total voltage across the circuit is distributed across the resistors as:

$$U_{\text{total}} = \sum_{i=1}^{n} U_i \tag{2}$$

Ohm's Law states that the current through the circuit, of an ideal case where there is no internal resistance of the circuit, is:

$$I = \frac{U_{\text{total}}}{R_{\text{eq}}} \tag{3}$$

The voltage across each resistor is proportional to its resistance:

$$U_i = I \cdot R_i \tag{4}$$

In a parallel circuit, the reciprocal of the equivalent resistance is the sum of the reciprocals of the individual resistances:

$$\frac{1}{R_{\text{eq}_p}} = \sum_{i=1}^{n} \frac{1}{R_i} \tag{5}$$

The voltage across each resistor is the same:

$$U_i = U_{\text{total}} \tag{6}$$

The current through each resistor is:

$$I_i = \frac{U_{\text{total}}}{R_i} \tag{7}$$

The total current is the sum of the branch currents:

$$I_{\text{total}} = \sum_{i=1}^{n} I_i \tag{8}$$

Where:

$$\begin{aligned} R_{\text{eq}_{s/p}} &= \text{Total equivalent resistance in the series/parallel circuit}(\Omega) \\ U_{\text{total}} &= \text{Total applied voltage across the series circuit}(V) \\ U_i &= \text{Voltage across the } i\text{-th resistor}(V) \\ I &= \text{Current through the circuit}(A) \end{aligned}$$

2.2 Voltage divider under Load

Consider the case of a circuit containing a voltage divider under load, two resistors, and an input voltage as shown in Fig. 4. The output voltage U_L across $R_{2\|L}$, using Eqs. 5 and 2, is given by:

$$U_{total} = I(R_1 + R_{2\|L})$$

$$I = \frac{U_{total}}{R1 + R_{2\|L}} \text{ , for no internal resistance.}$$

Substituting $R_{2\|L} = \frac{R_2 \cdot R_L}{R_2 + R_L}$ and knowing that $U_L = U_{total} = I \cdot R_1$, the equation becomes:

$$U_L = U \cdot \frac{\frac{R_2 \cdot R_L}{R_2 + R_L}}{R_1 + \frac{R_2 \cdot R_L}{R_2 + R_L}} \tag{9}$$

For $\frac{U}{U_L}$, it's obtained:

$$\frac{U}{U_L} = \left[R_1 + \frac{R_2 \cdot R_L}{R_2 + R_L} \right] \frac{R_2 + R_L}{R_2 \cdot R_L} \implies \frac{U}{U_L} = R_1 \cdot \frac{1}{R_L} + \frac{R_1}{R_2} + 1 \tag{10}$$

2.3 Wheatstone Bridge

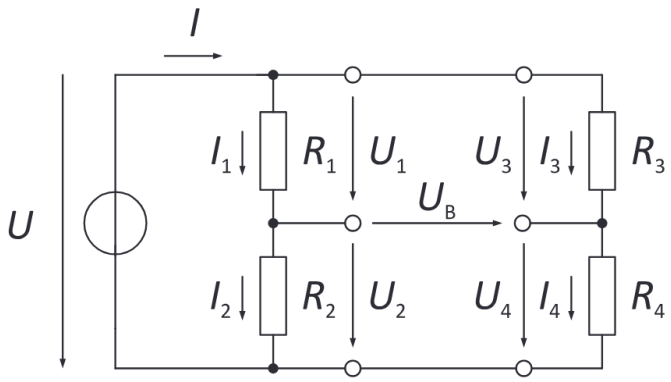

Figure 1: Wheatstone Bridge Circuit *Source:[5]*

The Wheatstone Bridge circuit, Fig. 1, is a combination of four resistors with connected by a bridge wire. It is commonly used, under the condition that the bridge voltage $U_b = U_c - U_d = 0$ where U_c and U_d are the voltages between $R_1 : R_2$ and $R_3 : R_4$ respectively. *Also put,* $R_1 = R_3$ *and* $R_2 = R_4$ as a means to measure the Ohms of an unknown resistor to a high degree of precision potentially in the $m\Omega$ with appropriate resistor values.

$$U_{out} = \frac{R_2}{R_1 + R_2} U_{in} \tag{11}$$

With this case and use of the voltage divider equation Eq.11 [2]:

$$\frac{R_2}{R_1 + R_2} = \frac{R_4}{R_3 + R_4} \tag{12}$$

Which results in a ratio of the resistances are ,when $U_b = 0$ or "balanced" [2] of:

$$\frac{R_1}{R_2} = \frac{R_3}{R_4} = 1 \quad \text{(Balanced)} \tag{13}$$

When R_4 is replaced with an unknown resistor and R_3 with a variable resistor. the initial deviation from this balanced state will result in a measurable deviation $U_b = 0$ however by setting the variable resistor to a value such that U_b is once again 0. R_4 can be determined as [2]:

$$R_4 = \frac{R_2 R_3}{R_1} \tag{14}$$

For the case that $U_b \neq 0$ for a known set of resistors U_b can be determined through use of Eq.11 and $U_b = U_c - U_d$ as:

$$U_b = U \left(\frac{R_2}{R_1 + R_2} - \frac{R_4}{R_4 + R_3} \right) \tag{15}$$

The Wheatstone Bridge's precise comparative method of resistive measurement also makes it very useful for resistive based sensors and also tackles the issue of thermal drift. Thermal drift occurs when the environmental temperature of a resistor can influence its measured resistance from tools such as a multimeter. However as the Wheatstone bridge is a comparative measurement between known resistors in the same environment this factor is accounted for leads to a more accurate measurement [3].

2.4 High Pass Filter

A High Pass Filter Fig., 11, is a circuit consisting of a capacitor, C, connected in series with a resistor, R, designed to allow high frequency signals to pass through the circuit, while reducing the amplitude, *or attenuating*, low frequency signals as they pass through. The distinction between what is a low or high frequency signal is determined by the cutoff frequency f_c [1].

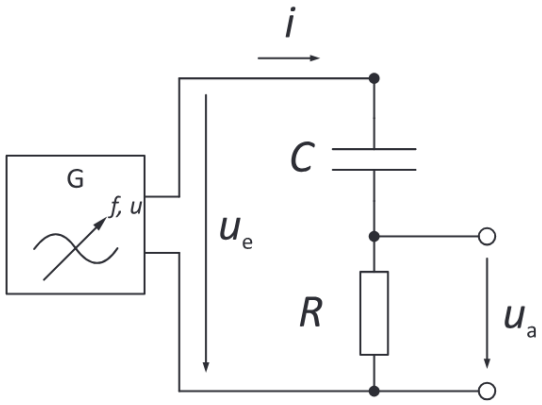

Figure 2: High Pass Filter Circuit *Source:[5]*

High pass filters are commonly used in scenarios where a reduction of low-frequency noise is needed, such as in audio processing, communication systems and image processing [1]. The output signal U_a is determined by the input voltage and the total impedance of the circuit [1].

$$U_a = U_e \frac{\frac{f}{f_c} i}{1 + \frac{f}{f_c} i} \tag{16}$$

Where:

$$f = \frac{1}{2\pi RC} = \text{Frequency } (Hz)$$
$$f_c = \text{Cut off frequency } (Hz)$$

Dividing Eq. 16 by U_e and taking the magnitude of the complex function leads to the transfer function:

$$\frac{U_a}{U_e} = \frac{\frac{f}{f_c}}{\sqrt{1 + \left(\frac{f}{f_c}\right)^2}} \tag{17}$$

The transfer function describes how the circuit modifies the incoming signal's amplitude and is useful, in conjunction with the cutoff frequency f_c to design a High Pass Filter for a specific use case. f_c is defined as the frequency at which the output amplitude is $\frac{1}{\sqrt{2}}$ of the input amplitude. Setting Eq. 17 to $\frac{1}{\sqrt{2}}$ one derive f_c as [1]:

$$f_c = \frac{1}{2\pi RC} \tag{18}$$

3 Experimental Setup

3.1 Basic Circuit

For task I, the circuit is built following the schemes shown in Fig. 3. The setup consists of three resistors, R_1, R_2, and R_3, connected in series with a voltage source U_{total}. The resistors are chosen to have different resistance values to observe their individual contributions to the circuit's behavior. Their values are $R_1 = 100.2 \pm 1.30\Omega$, $R_2 = 199.9 \pm 2.09\Omega$, $R_3 = 997.0 \pm 8.47\Omega$ and $U_{total} = 4.98 \pm 0.02V$. These values are used in both series and parallel setups. The voltages and intensities are measured by two digital multimeters, one placed at the input voltage (to avoid the internal resistance of the battery) and the other at each resistor.

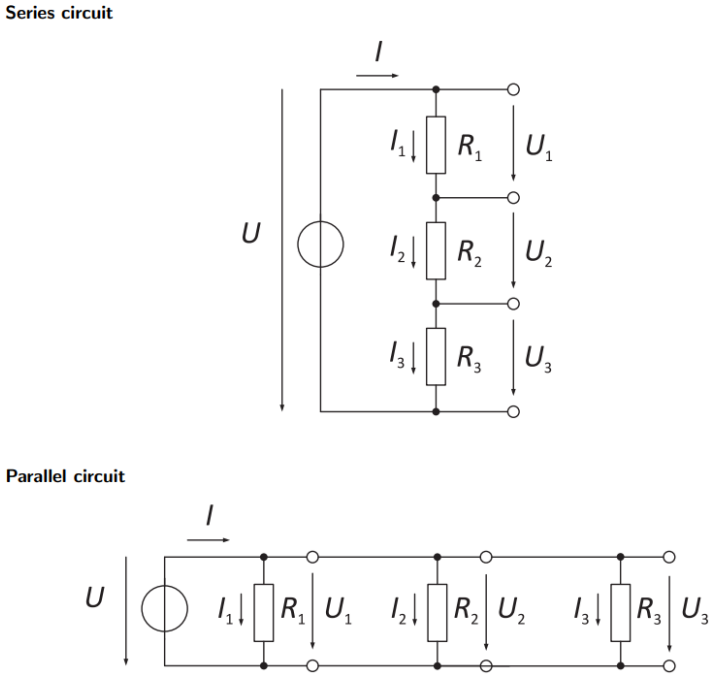

Figure 3: Task I - Schemes of the Circuits [5]

3.2 Voltage Divider under Load

For the second experiment, a voltage divider is placed in parallel with a resistor 2, which previously is connected in series with a resistor 1, as shown in Fig 4. In this case, the resistors are chosen to be $R_L \geq R_1 \parallel R_2$ (the equivalent resistance of R_1 and R_2 placed in parallel), $R_1 < R_2$ and in the limit of an unloaded voltage divider ($R_L \to \infty$) [5]. The multimeter placed at the input voltage remains unchanged and the other one is measuring the voltage through the divider, while its resistance is changing. For the accuracy of this experiment, the R_2 is fixed as $R_2 = 997.0 \pm 8.47\Omega$, while R_1 is calculated from the Eq. 10 and the measured values of the divider.

3.3 Wheatstone Bridge

The Wheatstone Bridge circuit was created in accordance to the circuit diagram Fig. 1 on a breadboard with through-hole components, a $R_1 = R_3 = (100.2 \pm 1.3016)\Omega$ and $R_2 = (997.0 \pm 10.98)\Omega$ was chosen, with R_4 chosen as a variable resistor, spanning a range of (100 - 9000Ω) such that it encompassed R_2 for comparison. For each value of R_4, U_a and U_e was recorded, and compared with theoretical results through use of Eq. 15.
A further non-linear analysis was performed on the collected data using Eq. 15 with the constraint that $R_1 = R_3$ and was compared with experimental data.

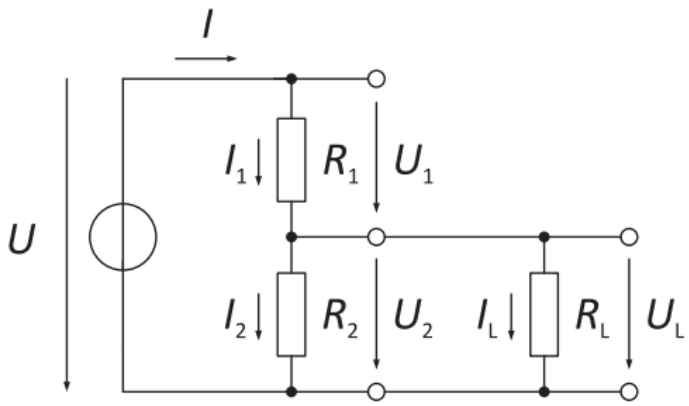

Figure 4: Task II - Schemes of the Circuit with Voltage Divider under Load [5]

3.4 High Pass Filter

The High Pass Filter circuit was created in accordance to the circuit diagram Fig.2 on a breadboard with through-hole components, a $R = (997 \pm 11)\Omega$ and $C = (5.81 \pm 0.35)nF$ were chosen resulting in an expected $f_c = (27.475 \pm 1.66)$Khz. U_e was originally set to 1.589V and through use of a PicoScope 2205A oscilloscope, the frequency f was varied from 100Hz to 100Khz, and U_e and U_a were recorded. It is of note that the uncertainty values for $\delta Ua = \delta U_e = 7.8125$mV, and $\delta f = 0.2$Hz were determined from the PicoScope 2000 Series Datasheet [4].

4 Data analysis

4.1 Basic Circuits

In Fig. 5, there are presented the voltages corresponding to different values of resistances connected in series. The graph pictures a linear relationship with an almost perfect fitting, for an equation with a corresponding slope $a = 0.00413$ and an intercept $b = -0.05$. This line fits with the three points scattered, with an $r^2 = 0.9998$. The experimental errors are plotted, but the values are small, almost not visible. The sum of other internal resistances are a total of $r_s \approx 0.1807\Omega$.

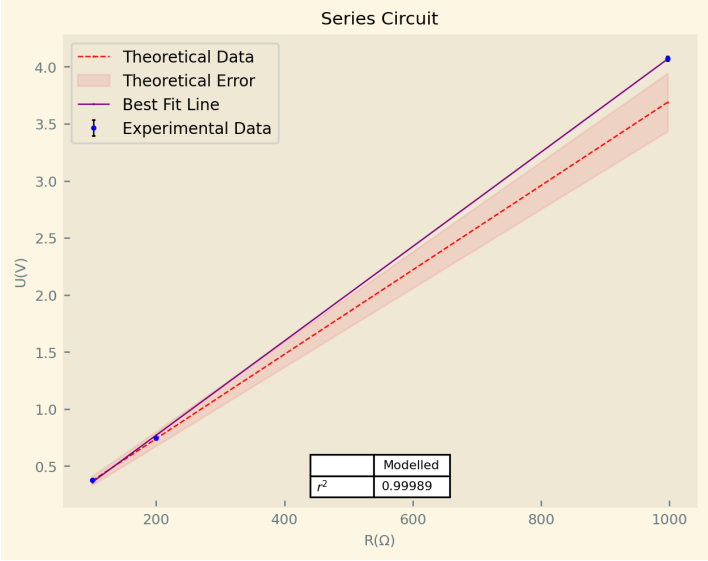

Figure 5: Series Circuit

In Fig. 6, the same three resistances are connected in parallel. Unlike the previous case, the graph

doesn't show a linear relationship. The slope of the graph is given as $a = 0.0008$, with an intercept of $b = 3.53$. This line doesn't fit the scattered points that gracefully, with an $r^2 = 0.81$. It is interesting to note that neither of the data points reaches the voltage of the battery, $U_{\text{total}} = 4.98 \pm 0.02V$, suggesting that there may be losses or other factors at play preventing the system from achieving the expected maximum voltage. The sum of other internal resistances are a total of $r_p \approx 0.36\Omega$. This value was calculated using the measured value of $R_1 = 100.2 \pm 1.30\Omega$, obtained prior to R_1 being installed in the circuit.

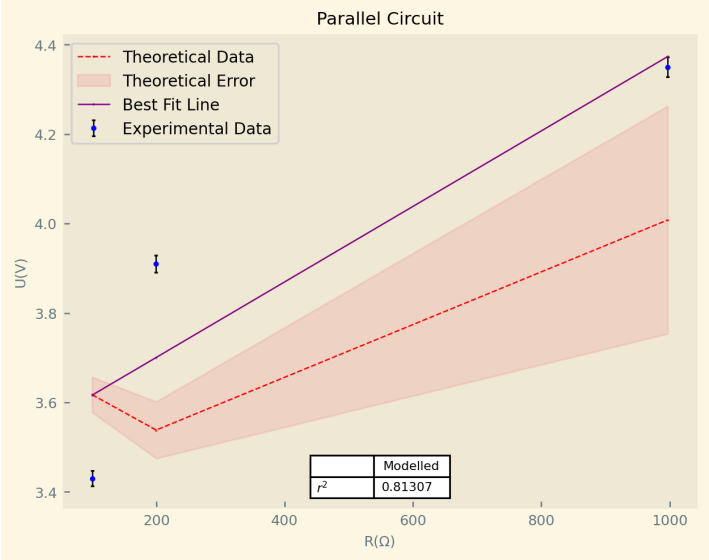

Figure 6: Parallel Circuit

4.2 Voltage Divider under Load

In this experiment, the first graph, shown in Fig. 7, illustrates the difference between the expected and actual data. Seeing that U maintains a fairly stable value, it is evident that for the largest values of R_L and U_L, the experimental results closely approach the theoretical values. This observation raises the question of whether the trend is inherent to the system or simply a result of improved accuracy with an increased number of measurements. In either case, it is clear that the internal resistance of the multimeters and from the cables plays a more significant role when R_L is smaller, producing the deviation between the experimental and theoretical values.

Focusing on the experimental data from the previous graph, Fig. 8 presents a linear fit of the best-fit line. This approach is used to accurately determine the value of R_1. By minimizing the deviation between the experimental points and the fitted line, this method ensures a precise estimation of R_1, accounting for any inherent uncertainties in the measurements. With a slope $a = 110.76$ and an intercept $b = 1.1115$, the line fits the experimental values with an $r^2 = 0.9999$. Considering Eq.10, x is substituted by $\frac{1}{R_L}$, with $a = R_1$ and $b = 1 + \frac{R_1}{R_2}$. This substitution results in $R_1 = 110.76\,\Omega$ and $\frac{R_1}{R_2} = 0.11$, thereby affirming the calculated value of R_1. The sum of other internal resistances are a total of $r \approx 10.56\Omega$.

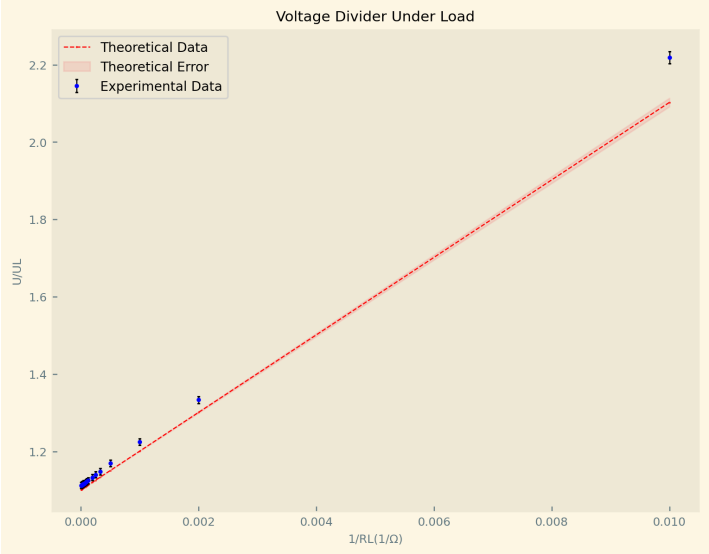

Figure 7: Theoretical and Experimental Data

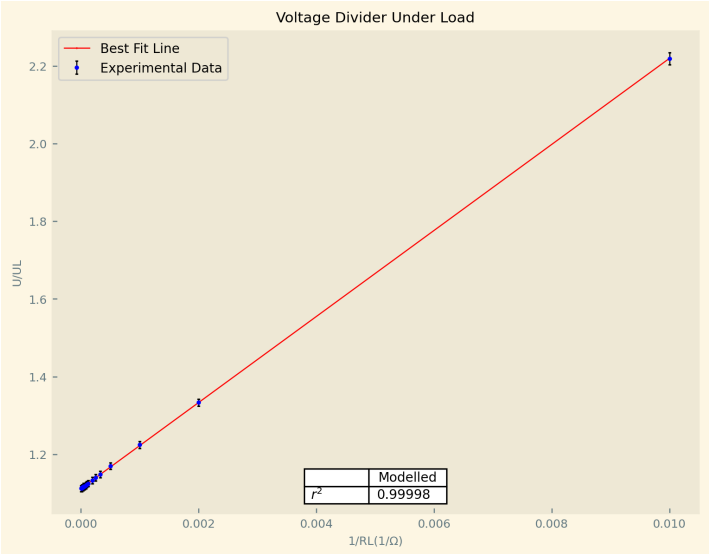

Figure 8: Linear Fitting of the R_1

4.3 Wheatstone Bridge

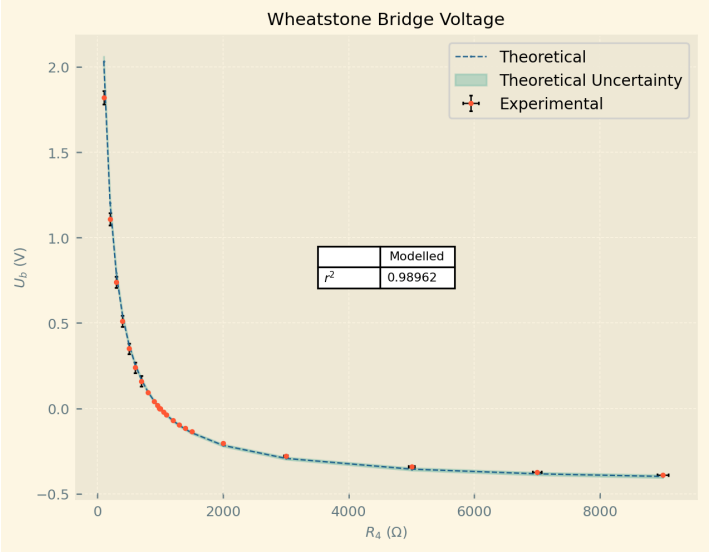

Figure 9: Wheatstone Bridge, Theory and Experimental

The experiment results of the Wheatstone bridge task is correlated strongly with the theoretical predictions, with an $r^2 = 0.9862$. Furthermore the theoretical uncertainty encompasses most of the experimental data points suggesting a high degree of accuracy.

It can be seen in Fig. 9 an increased density of recorded points about the point where $U_b = 0$ this was done increase the reliability of the measured data around the zero point as well compare the experimentally determined value for R_2 with measurement tools, as the Wheatstone Bridge is known for its precision. The exact value of $R_4 = R_2$ was unable to be as an increase of 1Ω resulted in a measured U_b step from $0.001V$ to $-0.0002V$. This jump is predicted to be a result of the resistance from the multimeter and the uncertainty,(1%) in the variable resistor device used. The range at which the measured value of R_2 exists is $(993 \pm 9.93 - 994 \pm 9.94)\Omega$. With such a high degree of uncertainty no definitive statements can be for or against the Multimeter measured value of $R_2 = (997.0 \pm 10.98)$.

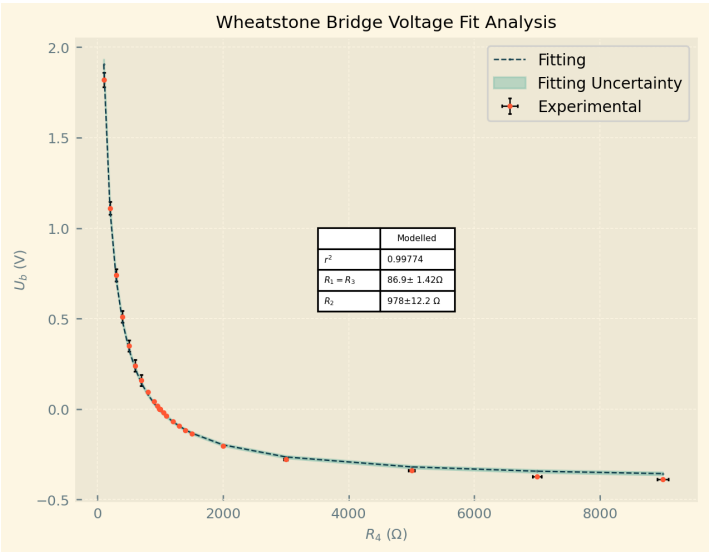

Figure 10: Wheatstone Bridge Non-Linear Fit

Fig.10 is a non-linear fit analysis on the experimental data through use of Eq. 15 with the constraint that $R_1 = R_3$. The results of the non-linear analysis found that the experimental data best fits theoretical expectations when $R_1 = R_3 = (86.9 \pm 1.42)\Omega$ and $R_2 = (978 \pm 12.2)\Omega$. As neither the analysis uncertainty in $R_1 = R_3$ or R_2 encompass the measured results it suggests a degree of inaccuracy in measured data or the influence of external factors.

4.4 High Pass Filter

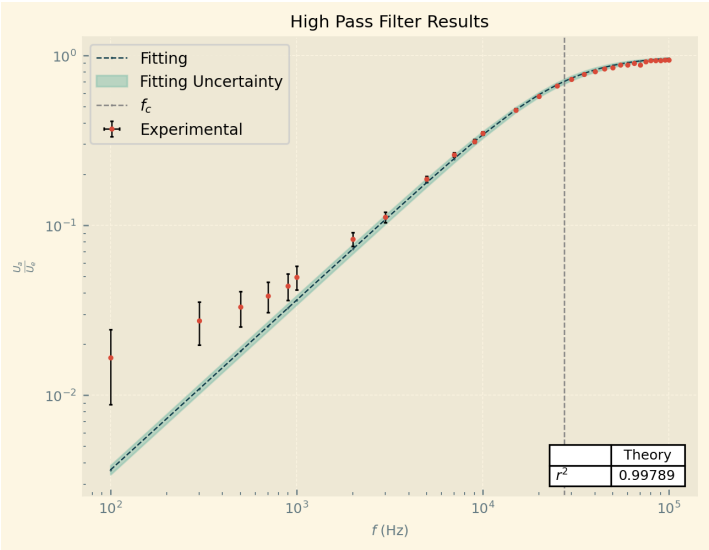

Figure 11: High Pass Filter Theory and Experimental

Overall the results of the High Pass Filter experiment, Fig.11 is in strong agreement with the theoretical expectations with a $r^2 = 0.99789$. The practical reduction of amplitude, or attenuation, of frequencies above $3000Hz$ are within the theoretical uncertainty, determined from Eq.17.

For frequencies below 3000Hz the attenuation was significantly lower than theoretical expectations as well as theoretical uncertainty, resulting in output frequencies that were higher than expected, these results are also not explained by the large relative uncertainty that these lower frequencies possess. It is predicted that this attenuation distortion is a result of a load impedance in the measurement device, the PicoScope 2205A, that paired with the total impedance of the circuit results in an impedance mismatch that in such a way that it significantly influences the output voltage of the circuit at low frequencies.

It should be noted that during the experiment it was noticed that the input voltage U_e decreased for higher frequencies, has not seemed to have affected the results of those data points and has been attributed to both thermal drift and a result of the PicoScope 2205A oscilloscope operating at higher frequencies.

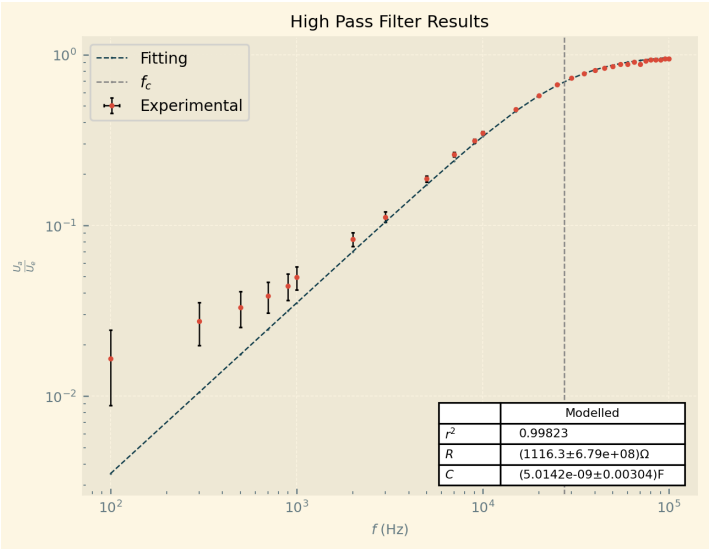

Figure 12: High Pass Filter Non-Linear Fit

A non-linear analysis with Eq. 17 on the experimental results of the High Pass Filter initially shows a stronger correlation of $r^2 = 0.99823$, with a determined theoretical $R = (1116.3 \pm 6.79 \cdot 10^8)\Omega$ and $C = (5.0142 \pm 3.04 \cdot 10^6)nF$, however taking into account the extremely large uncertainty of the determined R and C this value is wildly unreliable. The very large uncertainties in R and C were a result of error propagation through complex function and subsequently taking its magnitude. A comparison between values from experimentally chosen $R = (997 \pm 11)\Omega$ and $C = (5.81 \pm 0.35)nF$ is well within the fitted uncertainty however no comment on accuracy or precision of the experimentally chosen values $R = (997 \pm 11)\Omega$ and $C = (5.81 \pm 0.35)nF$ can be made, only that the fitted values are widely imprecise.

5 Discussion

These experiments don't represent ideal circuits, as each component introduces some degree of error or internal resistance. The first two tasks use linear fitting techniques to determine the most accurate values for key parameters, such as resistances. This approach helps to investigate the effects of experimental inaccuracies by focusing on the overall trends in the data, rather than individual deviations.

For Task I, fig. 5, the voltages for resistances connected in series show a nearly perfect linear relationship, with a slope of $a = 0.00413$ and an intercept of $b = -0.05$, resulting in $r^2 = 0.9998$. The experimental errors are small and nearly invisible. The total internal resistance is $r_s \approx 0.1807\Omega$, calculated by subtracting the voltages of each resistor from the input voltage U_{total}.
In Fig. 6, the three resistances are connected in parallel, and the graph deviates from a linear relationship. The slope is $a = 0.0008$ and the intercept is $b = 3.53$, with $r^2 = 0.81$. Notably, none of the data points reach the total battery voltage $U_{\text{total}} = 4.98 \pm 0.02V$, although getting closer with a higher value of the resistor. This is because the sum of internal resistances have a bigger impact on lower values of the resistors. The total internal resistance is $r_p \approx 0.36\Omega$, calculated using the the voltages measured at each resistor and subtracted them from the U_{total}.
Regarding the parallel circuit in Task I, the graph obtained deviates significantly from the expected results, suggesting the possibility of a human or experimental error. Several hypotheses were tested to improve the graph and identify the issue. These included considering whether the multimeter might have been incorrectly configured, which led to the calculation of a negative internal resistance; checking the order of magnitude of the data or investigating whether certain values were inputted incorrectly (e.g., due to a missing zero). Despite these efforts, the source of the discrepancy remains unclear. Therefore, repeating the experiment is necessary to ensure accurate data and proper fitting.

In task II, Fig. 7 shows the difference between expected and actual data. For larger R_L and U_L, experimental results align closely with theoretical predictions, likely due to reduced influence from internal resistances. For smaller R_L, the internal resistance of multimeters and cables causes deviations. Fig. 8 shows a linear fit with slope $a = 110.76$, intercept $b = 1.1115$, and $r^2 = 0.9999$. Using Eq. 10, where $x = \frac{1}{R_L}$, $a = R_1$, and $b = 1 + \frac{R_1}{R_2}$, the results yield $R_1 = 110.76\,\Omega$ and $\frac{R_1}{R_2} = 0.11$. The total internal resistance is $r \approx 10.56\Omega$, highlighting the impact of non-idealities in smaller R_L values.
By analyzing the relationship between theoretical and experimental data, the linear fits provide a method for estimating quantities like R_1 and verifying the underlying assumptions of the circuit models. Measuring different values for R_1 in the circuit, as compared to its value prior to being integrated into the circuit, doesn't imply that its resistance has changed. Instead, this discrepancy indicates that additional resistances within the circuit, such as internal resistances of multimeters or wiring resistances, are contributing to the total measured resistance. As well as for the difference between the theoretical values and the experimental ones accounts for the sum of the internal resistances of the cables and the resistances of the digital multimeters.

The experimental results of the Wheatstone Bridge task align strongly with theoretical predictions, 17 for the Wheatstone Bridge circuit with a high correlation coefficient ($r^2 = 0.9862$) between experimental and theoretical data, Fig. 9. Qualitatively, most experimental data points fall within the theoretical uncertainty suggesting a high degree of accuracy and precision. The results of Fig. 9, along with the measurement uncertainty in the variable resistor $\delta R_4 = 1\%$ used, made determination of R_2 via the Wheatstone Bridge circuit impractical as a data point at $U_b = 0$ was unable to be recorded, due to uncertainties resulting in a jump from $0.001V$ to $-0.0002V$. Experimentally R_2 was constrained to the range $(993 \pm 9.93)\,\Omega$ to $(994 \pm 9.94)\,\Omega$ overlapping with the multimeter's measurement of $((997.0 \pm 10.98)\Omega)$ but not definitively agreeing or disagreeing with the multimeter's measurement.

The non-linear analysis of the Wheatstone Bridge experimental data concluded that a stronger correlation of ($r^2 = 0.99774$) when $R_1 = R_3 = (86.9 \pm 1.42)\Omega$ and $R_2 = (978 \pm 12.2)\Omega$. However a qualitative examination of Fig.9 against 10 shows that this fitting favors the resistance values $R_4 < 2000\Omega$ with resistance values above this straying from the fitted curves uncertainty, contrasting with the theoretical predictions which have a more even distribution of values that fall in and outside of the theoretical curves uncertainty. What is also of note is that of the two fitted values $R_1 = R_3 = (86.9 \pm 1.42)\Omega$ and $R_2 = (978 \pm 12.2)\Omega$, the uncertainty in R_2 for both the fitted values and experimentally used

values, (978 ± 12.2) and (997.0 ± 10.98) respectively, overlap this could indicate that the Wheatstone Bridge circuit was able to more accurately determine a values for R_2, however due to the significant uncertainty in each value and placement of each value of R_2 at the fringes of uncertainty of each other this claim is spurious at best.
The conclusion of the Wheatstone Bridge experiment in this report remains inconclusive as to whether the accuracy of the circuit in comparison with digital measurement devices. For future endeavors it is recommended to a resistors and a variable resistor higher precision and a lower tolerances perhaps surface mounted resistors and potentiometer, and use of more precise electrical circuit than a breadboard, such as a PCB.
the experimental data obtained from the High Pass Filter task overall aligned strongly ($r^2 = 0.99823$) with the theoretical expectations. The overall trend of the data is consistent with theoretical literature and the determined $f_c = (27.475 \pm 1.66)$KHz is consistent with the experimental data. It is of note that further data collection beyond 100KHz was unable to be performed due to the AWG range of the PicoScope 2205A oscilloscope used.

For the High Pass Filter task it was observed that for frequencies above 3000Hz the experimental results lay within theoretical expectations. However for frequencies below 3000Hz there was an observed decrease in attenuation of the output frequency than theory suggests, resulting data points placed higher than the theoretical trend. This discrepancy is predicted to be a result of an interaction between the load impedance of the PicoScope 2205A interacting with the circuits total impedance and there being an impedance mismatch between the two. This impedance mismatch is such that its influence on the output voltage is significant for low frequency signals. This factor was not a consideration during the setup of the circuit, nor recording of data.

The non-linear fit performed on the High Pass Filter experimental data, Fig.12, resulted in a fitted stronger correlation of $r^2 = 0.99823$ for determined R, C of $(1116.3 \pm 6.79 \cdot 10^8)\Omega$ and $(5.0142 \pm 3.04 \cdot 10^6)$nF respectively. However when considering the very large uncertainty in the fitted values of R and C the correlation determined possess almost no precision, and is thus unreliable. The large uncertainties in the fitted R and C is a result of the use of the complex function Eq.17 and the error propagation through computation and taking the magnitude of the complex function.

In future study into the High Pass Filter circuit it is recommended to conduct to the experiment using more precise, SMD, components on a electric board that is less prone to external resistances and impedance, such as a specialized PCB board.

References

[1] R. A. e. a. A. Muthali, N. Ramachandran. Note 6b: Transfer functions. https://eecs16b.org/notes/sp24/note06B.pdf, 2022. Accessed: 8-12-2024.

[2] ElectronicsTutorials. Wheatstone bridge. https://www.electronics-tutorials.ws/blog/wheatstone-bridge.html, 2023. Accessed: 8-12-2024.

[3] H. B. . Kjær. Strain gauges: How to prevent temperature effects on your measurement. https://www.electronics-tutorials.ws/filter/filter_3.html, 2024. Accessed: 8-12-2024.

[4] P. Technology. Picoscope 2205a series oscilloscope datasheet, 2024. URL https://www.picotech.com/download/datasheets/picoscope-2000-series-data-sheet-en.pdf. Accessed: 10-12-2024.

[5] M. Ziese. *E1e Basic Electric Circuits*. Universität Leipzig, December 2024.